

# **ICPES 2025**

40<sup>th</sup> INTERNATIONAL CONFERENCE ON PRODUCTION ENGINEERING - SERBIA 2025

DOI: 10.46793/ICPES25.172B



University of Nis
Faculty of Mechanical
Engineering

Nis, Serbia, 18 - 19th September 2025

# NANOCORROSION EFFECT ON NITI ARCHWIRE EXPOSED TO VARIOUS MOUTHWASHES

Zoran BOBIĆ<sup>1\*</sup>, Lazar KOVAČEVIĆ<sup>1</sup>, Vladimir TEREK<sup>1</sup>, Marko ZAGORIČNIK<sup>1</sup>, Sanja KOJIĆ<sup>1</sup>, Goran STOJANOVIĆ<sup>1</sup>, Bojan PETROVIĆ<sup>2</sup>, Pal TEREK<sup>1</sup>

Orcid:0000-0002-0843-4984; Orcid:0000-0002-4087-4373; Orcid:0000-0002-4764-3172; Orcid: 0000-0002-4092-9733; Orcid: 0000-0003-2098-189X; Orcid: 0000-0002-3575-3921; Orcid: 0000-0001-9994-6039;

<sup>1</sup>University of Novi Sad, Faculty of Technical Sciences, Novi Sad, Serbia

<sup>2</sup>University of Novi Sad, Faculty of Medicine, Novi Sad, Serbia

\* Corresponding author: zoranbobic@uns.ac.rs

Abstract: Nitinol is widely used for orthodontic archwires due to its favourable mechanical properties and corrosion resistance. To maintain oral hygiene and prevent dental plague, orthodontic patients are advised to use commercially available mouthwashes, many of which contain chlorine- or fluorine-based compounds. These compounds can interact with the surface oxide layer of NiTi alloy, potentially leading to its degradation and the release of toxic nickel ions into the surrounding biological environment. The detrimental effects of chlorine- and fluorine-containing media on NiTi are well-known. However, due to the typically low intensity of the corrosion processes, the characterization of surface corrosion effects in such environments remains a great challenge. In this study, non-electrochemical corrosion tests were conducted on NiTi archwires exposed to artificial saliva and several commercially available mouthwashes to quantify nanometric changes in surface topography. Corrosion effects were evaluated using atomic force microscopy (AFM) in contact mode, with measurements taken at predefined surface locations before and after the corrosion tests. The topographical changes were evaluated using surface roughness parameters: Sa, Ssk, Sdr, and S10z. The analysis revealed that mouthwashes containing chlorine compounds resulted in both material loss and gain on the surface, while fluorine-based mouthwashes caused only material loss. In contrast, samples exposed to artificial saliva exhibited no significant topographical changes. The analytical approach developed in this study proves effective for identifying and distinguishing types of nanoscale surface alterations associated with corrosion. The observed material gain in chlorine-containing mouthwashes is likely due to surface reoxidation, a phenomenon not present in fluorine-containing solutions.

Keywords: NiTi, Corrosion, Mouthwashes, Artificial Saliva, AFM, Nano topography

## 1. INTRODUCTION

Nickel-titanium (NiTi) alloy is a biomaterial widely used in dental orthodontic applications. During orthodontic treatment, practitioners often recommend that patients use various mouthwashes to prevent caries and protect

dental enamel [1]. As a result, NiTi wires are exposed to different oral environments that may lead to corrosion and the release of metal ions into the body. The release of these ions can have adverse biological effects, depending on the ion species and their concentrations [2].

Corrosion resistance is a critical property of biomaterials, as it directly influences their biocompatibility. It has been shown that nickel ion release, caused by corrosion processes, can lead to allergenicity, toxicity, and even carcinogenicity [1,2]

Evaluating the corrosion behavior of NiTi alloys under conditions similar to those in the human oral cavity remains a significant characterization challenge. Many studies [3–6] avoid the complexities of characterizing nanostructures and nanoscale surface changes by employing accelerated corrosion tests. However, such tests do not accurately replicate real clinical conditions.

Therefore, the aim of this work was to perform non-accelerated corrosion tests on NiTi wires in various corrosive media and to characterize and quantify the resulting topographical changes. To achieve this, atomic force microscopy (AFM) measurements were conducted before and after the corrosion tests.

#### 2. EXPERIMENTAL

The corrosion performance of NiTi orthodontic wires (Dentaurum, Germany) was evaluated in this study. Four prismatic specimens were prepared from the as-received wire. Prior to the corrosion tests, six scan locations were marked on each specimen. To facilitate the relocation of the same areas after corrosion testing, the scan sites were identified by making small scratches on the specimen surface. Returning to the same locations after testing allows for the characterization of nanotopographic changes induced by corrosion with a relatively low number of measurements. In contrast, detecting such changes through randomly selected areas would require a significantly larger number of measurements, both before and after corrosion. Each specimen was exposed to one of four selected corrosive media (artificial saliva or commercial mouthwash).

Corrosion was characterized by analyzing changes in surface topography. For this purpose, each specimen was examined at six

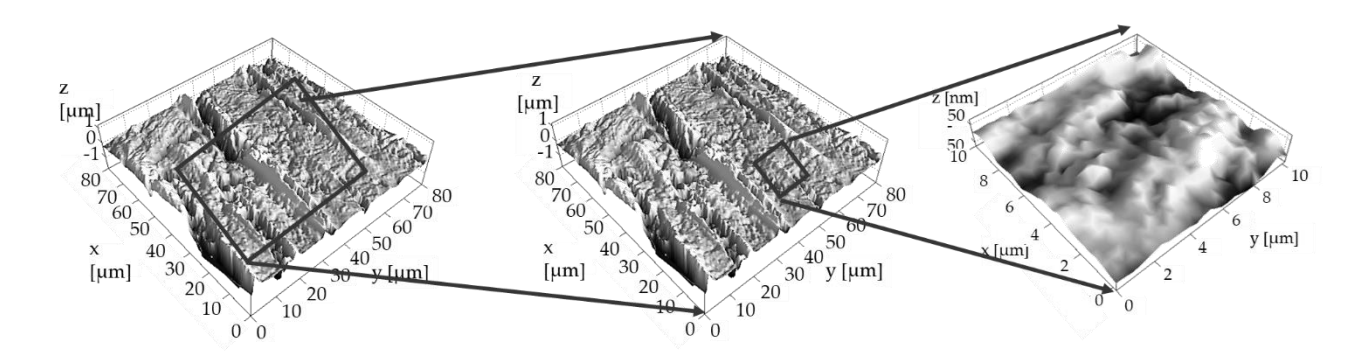
predefined locations before and after the corrosion test using atomic force microscopy (AFM; CP-II di, Veeco). AFM measurements were conducted in contact mode using a symmetrically etched silicon nitride tip. The scanning parameters were as follows: fast scanning direction along the X-axis, scanning area of  $100 \times 100 \ \mu m$ , setpoint of 225 nN, scanning rate of 0.5 Hz, and gain of 0.5.

Table 1. Sample denotation

Sample	Corrosive medium
Sample 1	Artificial Saliva
Sample 2	Aquafresh® Mouthwash
Sample 3	Eludril® Mouthwash
Sample 4	Listerine® Mouthwash

To enable accurate repositioning of the probe after the corrosion test, a specific procedure was developed. Before and after testing, the probe was positioned relative to the specimen using a predefined probe elevation to maintain consistency in the probe/sample alignment. However, during the approach of the probe to the sample surface, deviations from the ideal path were occasionally observed. These deviations may lead to slight mismatches in scanning location before and after corrosion exposure. Therefore, the exact probe path was determined both before and after the corrosion test. Based on differences in probe trajectories and specimen height variations, probe position corrections were calculated. However, even this procedure could not guarantee repositioning of the probe at identical locations following corrosion exposure. To address this,  $80 \times 80 \mu m$  and  $10 \times 10 \mu m$  sub-areas were extracted from the original 100 x 100 µm scanned regions. The effects of corrosion were evaluated within these extracted areas.

Topographic image analysis was conducted using SPIP software (Image Metrology), which was used to extract the  $80 \times 80 \, \mu m$  and  $10 \times 10 \, \mu m$  regions and calculate surface roughness parameters. All quantitative parameters obtained from the AFM measurements were first subjected to a normality test (Anderson–Darling test, p > 0.05), followed by a paired t-



**Figure 1.** Characteristic surface topography image of NiTi with the marked location used for evaluating corrosion effects.

test. Statistical analyses were performed using Minitab 16 software at a significance level of 5%. test. Statistical analyses were performed using Minitab 16 software at a significance level of 5%.

#### 3. RESULTS

Representative topography images of NiTi surface before corrosion test are presented in Figure 1. The NiTi surface exhibits characteristic parallel grooves with smooth areas between them, a pattern resulting from the manufacturing process.

Representative AFM topography images of Sample 3 before and after the corrosion test are presented in Figure 2. A comparison of these two images reveals slight nano scale changes in surface topography following the corrosion test.

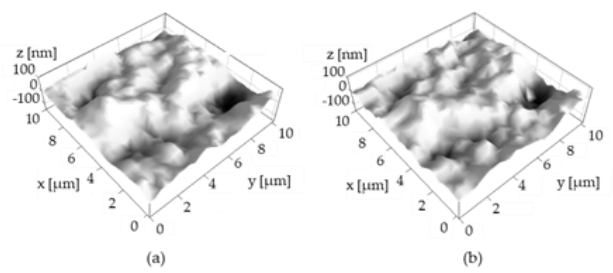


**Figure 2.** Representative AFM topography images of Sample 3: (a) before and (b) after the corrosion test.

Figures 3 and 4 present the calculated surface roughness parameters over a 10  $\mu$ m  $\times$  10  $\mu$ m area, both before and after corrosion testing. Prior to corrosion, all samples showed Sa values between 10–30 nm and S10z values ranging from 80–180 nm, indicative of a nearly

polished surface state (Figure 2). Following the corrosion test, slight changes in Sa and S10z were observed, with statistically significant differences detected in Samples 2, 3, and 5.

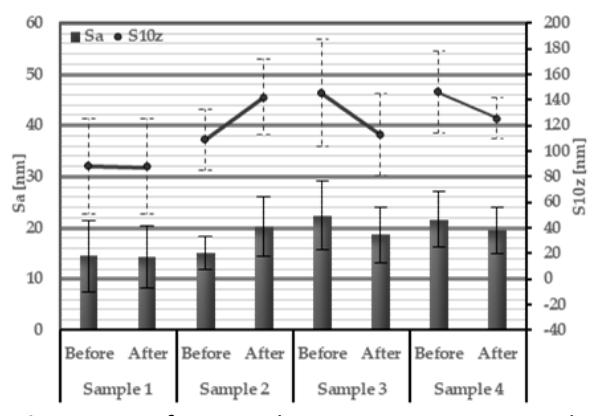


**Figure 3.** Surface roughness parameters Sa and S10z before and after the corrosion test.

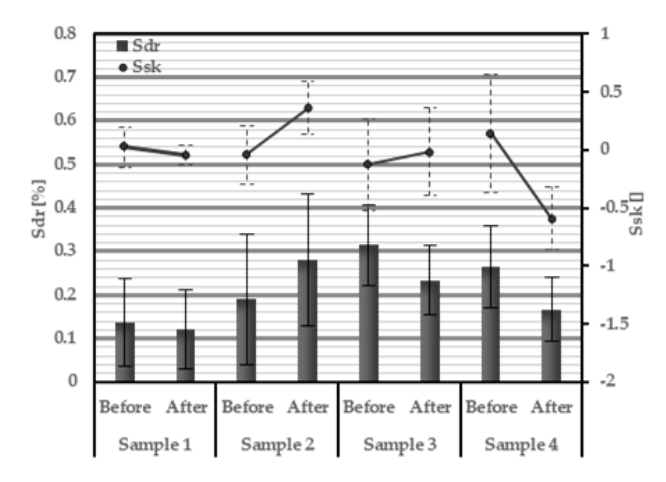


**Figure 4.** Surface roughness parameters Sdr and Ssk before and after corrosion test

Figure 3 shows the results for the Sdr and Ssk parameters. Before corrosion, the Ssk values were low, indicating a uniform surface without prominent protrusions or grooves. Similarly, the Sdr values were close to zero, reflecting a relatively flat surface with minimal deviation

from an ideal smooth profile, i.e., minimal surface protrusions or pits. After corrosion testing, changes in both Ssk and Sdr were observed. These changes were statistically significant for Sample 2 and 4 with respect to the Ssk parameter, and for Samples 2, 3, and 4 with respect to the Sdr parameter.

#### 4. DISCUSSION

The changes observed in surface topography over 10 × 10  $\mu$ m areas for samples treated with mouthwashes (Samples 2, 3, and 4) indicate that the corrosion processes induced nanoscale alterations. These findings confirm that the corrosion effects were of very low intensity and could only be statistically discerned in regions with low initial surface roughness. In this study, such regions were identified exclusively within surface segments of 10 × 10  $\mu$ m.

The results of statistical analysis revealed that samples exposed to the investigated mouthwashes (Samples 2, 3, and 4) exhibited statistically significant changes in nearly all analyzed surface roughness parameters. These, observed changes are consistent with findings from previous studies where it was shown that the presence of fluoride and chloride ions leads to reduced corrosion resistance [1,4,5,7–10], change in surface morphology [1,5,7,8,10], and increased nickel ion release from NiTi alloys [9,11–14].

To determine whether the corrosion caused by specific media led to material loss, gain, or both, it was necessary to assess the changes relative to the surface mean plane. In this study, a methodology was developed for evaluating material gain or loss by analyzing the combined changes in various surface roughness parameters. The underlying logic behind the developed methodology is explained on an exemplary surface and graphically presented in Figure 5. The initial surface was approximated by a sinusoidal profile with minor peaks and valleys distributed around the mean plane (Figure 5a). The possible effects of corrosion and the locations of their manifestation on the initial profile are schematically represented by symbols given in Figure 5b. After incorporating these transformations, a profile model is obtained. It contains all the changes that may occur on the initial profile (Figure 5c). By analyzing the formulas used to calculate them, the change in each surface roughness parameter (Sa, Sdr, Ssk) can be correlated with a specific dominant corrosion effect, i.e., material gain or loss relative to the mean profile plane. Through an elimination-based approach, effects that produce contradictory trends in the roughness parameters can be excluded. This enables the identification of the predominant corrosion mechanism acting on each sample.

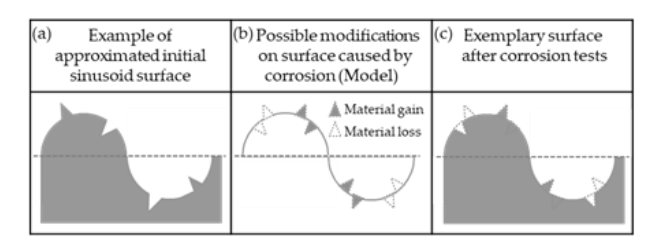


Figure 5. Graphical presentation of the analysis performed for detection of corrosion effects on surface topography: (a) approximated initial profile (before treatment); (b) possible corrosion effects and their locations; (c) profile of exemplary surface after corrosion.

The analysis begins with the evaluation of changes in the Sa parameter, as illustrated in Figure 6. An increase in Sa, as observed for Sample 2, may result from either material gain above the mean plane and/or material loss below it. All other potential effects would lead to a reduction in Sa and are therefore considered non-dominant. Conversely, the decrease in Sa observed for Sample 3 suggests the presence of material loss above and/or material gain beneath the mean plane. Sample 4 did not exhibit a detectable change in the Sa parameter, which means that in this medium all corrosion effects can be present on the surface.

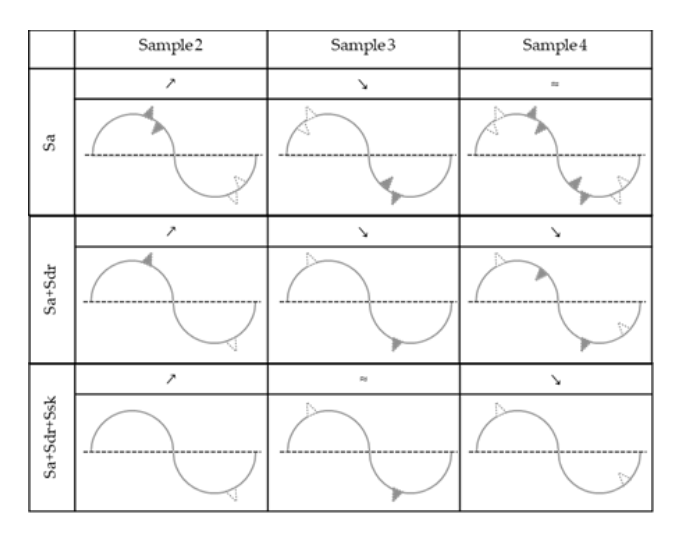


Figure 6. Determining the main corrosion effects. The empty triangle (material loss) vs. the full triangle (material gain). The statistical results are indicated by the following symbols: ≈, ↗, ∠. These symbols represent: insignificant difference, significant increase, and significant decrease in parameters.

The Sdr parameter for Sample 2 also increased following the corrosion test, implying that effects which would reduce the developed surface area can be excluded as dominant mechanisms. The concurrent increase in both Sa and Sdr values in Sample 2 is thus consistent with corrosion-induced material gain above the mean plane and/or material loss beneath it. A similar analytical approach was applied to Samples 3 and 4, and the findings are also presented in Figure 6.

The analysis of corrosion-induced changes in the Ssk parameter is inherently more complex. It is well established that high positive Ssk values indicate a surface dominated by peaks above the mean plane, and vice versa [42]. However, due to the high sensitivity of this parameter, its variations cannot be directly or linked to specific corrosion clearly a mechanism. For instance, significant changes in Ssk may result from relatively low-intensity alterations at peaks or valleys located far from the mean plane. Conversely, high-intensity changes in the surface topography may shift the position of the mean plane relative to otherwise unchanged features, thereby amplifying the apparent prominence of a large number of peaks or valleys. Nonetheless, it was possible to discern a previous effect by

observing a change in Sa parameter. It can be reasonably proposed that a significant change will inevitably lead to a repositioning of the mean plane. Consequently, in the event of a substantial change in the Ssk parameter, it is possible to deduce whether this change is primarily the result of mean plane repositioning or a consequence of low-intensity, localized corrosion effects on the surface profile.

For Sample 2, an increase in both Sa and Ssk was observed. In consideration of the preceding analysis, it can be determined that the corrosion resulted in material loss on the surface. Furthermore, it can be deduced that all other possible effects are negligible. A similar analysis was performed, and it was determined that a dominant corrosion effect was present for all of the investigated media. The results of this analysis are presented in Figure 13. The analysis revealed that treatments with fluoridecontaining media, namely Aquafresh® (Sample 2) and Listerine® (Sample 4), caused material loss, while fluoride-containing Eludril® (Sample 3) caused both material loss above the mean plane and/or material gain beneath the mean plane.

### 5. CONSLUSION

This investigation evaluated the topographic changes of NiTi alloy archwires exposed to artificial saliva and fluorine- and chlorine-containing mouthwashes. The following conclusions can be drawn from the results obtained:

- The sample exposed to artificial saliva did not display statistically significant changes in any surface roughness parameter.
- A new analysis method was developed to identify material gain or loss based on surface roughness parameters. It revealed that fluoride mouthwashes (Aquafresh® and Listerine®) cause material loss, while chlorine mouthwashes (Eludril®) can cause both gain and loss.

#### **REFERENCES**

- [1] N. Schiff, B. Grosgogeat, M. Lissac, F. Dalard, M." Ele Lissac, F. Dalard, Influence of fluoridated mouthwashes on corrosion resistance of orthodontics wires, Biomaterials. 25 (2004) 4535–4542. https://doi.org/10.1016/j.biomaterials.2003.11.042.
- [2] R. Köster, D. Vieluf, M. Kiehn, M. Sommerauer, J. Kahler, S. Baldus, T. Meinertz, C.W. Hamm, Nickel and molybdenum contact allergies in patients with coronary in-stent restenosis, Lancet. 356 (2000) 1895–1897. https://doi.org/10.1016/S0140-6736(00)03262-1.
- [3] X. Li, J. Wang, E. Han, W. Ke, Influence of fluoride and chloride on corrosion behavior of NiTi orthodontic wires, Acta Biomater. 3 (2007) 807–815. https://doi.org/10.1016/j.actbio.2007.02.00 2.
- [4] H.H. Huang, T.H. Lee, T.K. Huang, S.Y. Lin, L.K. Chen, M.Y. Chou, Corrosion resistance of different nickel-titanium archwires in acidic fluoride-containing artificial saliva, Angle Orthod. 80 (2010) 547–553. https://doi.org/10.2319/042909-235.1.
- [5] P. Osak, B. Łosiewicz, EIS Study on Interfacial Properties of Passivated Nitinol Orthodontic Wire in Saliva Modified with Eludril® Mouthwash, Prot. Met. Phys. Chem. Surfaces. 54 (2018) 680–688. https://doi.org/10.1134/S20702051180402 26.
- [6] G. Perinetti, L. Contardo, M. Ceschi, F. Antoniolli, L. Franchi, T. Baccetti, R. Di Lenarda, Surface corrosion and fracture resistance of two nickel-titanium-based archwires induced by fluoride, pH, and thermocycling. An in vitro comparative study, Eur. J. Orthod. 34 (2012) 1–9. https://doi.org/10.1093/ejo/cjq093.
- [7] X. Li, J. Wang, E. hou Han, W. Ke, E. hou Han, W. Ke, E. hou Han, W. Ke, Influence of fluoride and chloride on corrosion behavior of NiTi orthodontic wires, Acta Biomater. 3

- (2007) 807–815. https://doi.org/10.1016/j.actbio.2007.02.00 2.
- [8] E.J. Kassab, J.P. Gomes, Assessment of nickel titanium and beta titanium corrosion resistance behavior in fluoride and chloride environments, Angle Orthod. 83 (2013) 864– 869. https://doi.org/10.2319/091712-740.1.
- [9] N. Schiff, M. Boinet, L. Morgon, M. Lissac, F. Dalard, B. Grosgogeat, Galvanic corrosion between orthodontic wires and brackets in fluoride mouthwashes, Eur. J. Orthod. 28 (2006) 298–304. https://doi.org/10.1093/ejo/cji102.
- [10] S. Kožuh, L. Vrsalović, M. Gojić, S. Gudić, B. Kosec, Comparison of the corrosion behavior and surface morphology of niti alloy and stainless steels in sodium chloride solution, J. Min. Metall. Sect. B Metall. 52 (2016) 53–61. https://doi.org/10.2298/JMMB150129003K
- [11] C.M. Ogawa, K. Faltin, F.A. Maeda, C.L.F.F. Ortolani, R.O. Guaré, C.A.B.B. Cardoso, A.L.F.F. Costa, In vivo assessment of the corrosion of nickel–titanium orthodontic archwires by using scanning electron microscopy and atomic force microscopy, Microsc. Res. Tech. 83 (2020) 928–936. https://doi.org/10.1002/jemt.23486.
- [12] E.O. Nasakina, M.A. Sudarchikova, K. V. Sergienko, S. V. Konushkin, M.A. Sevost'Yanov, Ion release and surface characterization of nanostructured nitinol during long-term testing, Nanomaterials. 9 (2019).
  - https://doi.org/10.3390/nano9111569.
- [13] P. Močnik, T. Kosec, J. Kovač, M. Bizjak, The effect of pH, fluoride and tribocorrosion on the surface properties of dental archwires, Mater. Sci. Eng. C. 78 (2017) 682–689. https://doi.org/10.1016/j.msec.2017.04.05 0.
- [14] A. Mirhashemi, S. Jahangiri, M. Kharrazifard, Release of nickel and chromium ions from orthodontic wires following the use of teeth whitening mouthwashes, Prog. Orthod. 19 (2018) 4. https://doi.org/10.1186/s40510-018-0203-7.